Highly Spin-Polarized Photoemission near Threshold from Physisorbed Xenon and Krypton Atoms

G. Schönhense, A. Eyers, U. Friess, F. Schäfers, and U. Heinzmann
Fritz-Haber-Institut der Max-Planck-Gesellschaft, D-1000 Berlin 33, West Germany
(Received 18 October 1984)

By use of circularly polarized synchrotron radiation at BESSY, spin-polarized photoemission from the valence orbitals of Xe and Kr atoms adsorbed on the Pt(111) single-crystal surface has been studied. Under certain conditions almost complete photoelectron polarization parallel or antiparallel to the photon spin was observed, allowing a direct assignment of quantum numbers of the states involved. Highly resolved intensity and polarization spectra in the threshold region exhibit pronounced variations versus photon energy.

PACS numbers: 32.80.Fb, 71.70.Ej, 79.60.Gs

Energy- and spin-resolved photoemission from free rare-gas atoms has been studied extensively during the past few years,[1] because it provides independent information in addition to the cross section. The major achievement of this new type of measurement has been the full quantum-mechanical characterization of the photoionization process.[2] As a result of the development of electron storage rings it has now become possible to extend angle-resolved photoelectron polarization spectroscopy to atoms in the adsorbed phase. A first theoretical model calculation for spin-polarized adsorbate photoemission has previously been carried out by Feder,[3] who predicted high degrees of photoelectron polarization and demonstrated the capability of the method to yield new information on the symmetry (i.e., the quantum numbers) of the states involved and also on the adsorption geometry. In this Letter we present the first experimental spin-polarization data for adsorbate photoemission. For the first study the physisorbed rare gases Xe and Kr seemed favorable, because spin-polarization effects in the gas phase are well known, the atoms are only weakly affected by the substrate, and detailed photoelectron spectroscopy work exists.[4–6]

Gas-phase photoionization of Xe $5p^6(^1S_0)$ ($4p$ for Kr) leads to Xe^+ $5p^5(^2P_{3/2,1/2})$ called the $p_{3/2}$ and $p_{1/2}$ hole states and separated by the spin-orbit splitting of 1.31 eV (0.66 eV for Kr). Waclawski and Herbst[4] concluded from Xe adsorbate photoemission spectra that $^2P_{3/2}$ is split into two different components attributed to the lifting of the $|m_j|$ degeneracy. The energetic ordering of the $|m_j|=\frac{3}{2}$ and $\frac{1}{2}$ sublevels has since been the subject of much controversial discussion (for a recent summary, see Ishi and Ohno[7]), because the ordering is indicative of the splitting mechanism. Whereas Waclawski and Herbst[4] suggested that the splitting was due to substrate-induced relaxation effects in the final ionic state, Horn, Scheffler, and Bradshaw[5] concluded that lateral interactions in the adlayer were responsible. The latter explanation has been challenged repeatedly in recent years.[6]

Applying the density-matrix formalism we have derived the photoelectron polarization P_z along the photon spin as a function of the radial dipole matrix elements. In the special case of emission along the photon impact direction ($\theta=\pi$), the matrix elements cancel out, yielding

$$P_z(\theta=\pi)=\begin{cases}-1 & \text{for } p_{3/2}, \quad |m_j|=\frac{3}{2},\\ +1 & \text{for } p_{3/2}, \quad |m_j|=\frac{1}{2},\\ +1 & \text{for } p_{1/2}.\end{cases} \tag{1}$$

It is informative to compare these results with the free-atom case: For $p_{1/2}$ they are identical and the complete positive polarization has already been observed in a recent gas-phase experiment.[1] The degeneracy of the two $p_{3/2}$ levels in free ions leads to values close to $P_z=-0.5$ since the intensity ratio between the $|m_j|=\frac{3}{2}$ and $\frac{1}{2}$ channels is close to 3 (exactly 3 in the LS-coupling approximation). Hence we find that for $p_{3/2}$ the adsorbed Xe atoms can emit photoelectrons with a degree of spin polarization considerably higher than do free Xe atoms. This difference is due to lifting of the degeneracy of the $p_{3/2}$ sublevels on the substrate. Furthermore, from the energetic ordering of the levels with positive and negative polarization, it is evident which $|m_j|$ value corresponds to the state with the lowest binding energy.

The experimental setup used recently for spin-polarized photoemission spectroscopy of Pt(111)[8] was supplied with a liquid-He–cooled target manipulator. The adsorbate was introduced via a doser nozzle which kept the background pressure below 10^{-9} mbar (base pressure 5×10^{-11} mbar), allowing the continuous monitoring of the spectra and LEED pattern as a function of coverage. In agreement with a recent study[9] of Xe on Pt(111) we observed sharp LEED spots from a $(\sqrt{3}\times\sqrt{3})R30°$ commensurate overlayer for Xe and Kr, corresponding to an adatom spacing of 4.80 Å. At higher coverages the layers are compressed to hexagonally close-packed (hcp) incommensurate monolayers (Xe-Xe spacing 4.35 ± 0.05 Å just before second layer growth, $T\sim55$ K). The transition from the com-

mensurate to the incommensurate Xe layer was observed also for the first time in the highly resolved photoelectron intensity spectra (cf. Fig. 1, spectra $a-i$). Peak positions and sublevel splittings differ significantly in the $\sqrt{3}$ and hcp overlayer (spectra d and i, respectively) demonstrating the substantial influence of the valence-orbital overlap on level positions and splittings.[5] The second and third layers give rise to photoemission peaks shifted to higher binding energies (spectra l,m,n) as observed by Mandel, Kaindl, and Schneider.[6]

Two spin-resolved photoelectron spectra are shown in Fig. 2, illustrating the method of spin-polarization measurements. For Xe and Kr the peak at lowest binding energy (peak 1) has nearly complete negative spin polarization which, according to Eq. (1), corresponds to the $p_{3/2}$, $|m_j| = \frac{3}{2}$ hole state, whereas peak 2 and peak 3 (here for Kr only) are highly positively polarized, i.e., $|m_j| = \frac{1}{2}$. This result confirms the peak assignment given by Horn, Scheffler, and Bradshaw,[5] which indicates that the splitting is caused by lateral Xe-Xe interactions.

The photoelectron spectra at low photon energies are strongly dominated by the adsorbate photoemission which can exceed the Pt d-band emission (close to E_F) by two orders of magnitude! In order to study the threshold behavior in more detail, we have measured the energy variation of peak intensities and polarizations (the underlying background of unpolarized secondary electrons from Pt causes a slight reduction of the measured polarizations). It is advantageous to plot the data versus photon energy because this representation is well defined independent of work-function changes. Figure 3 summarizes the results for incommensurate hcp layers of Xe and Kr and the commensurate Xe $\sqrt{3}$ layer. The upper figures reveal that the intensities of all peaks are strongly enhanced just above their thresholds (binding energies with respect to the vacuum level) but fall off rapidly towards higher energies. The photoelectron polarizations exhibit pronounced variations. One striking feature is the sharp minimum in the $|m_j| = \frac{3}{2}$ channel for Xe hcp at 11.7 eV, accompanied by a minimum in the corresponding intensity (solid curve, upper figure). For the commensurate Xe $\sqrt{3}$ layer, however, the minimum does not occur such that on dosing with a little more Xe to the $\sqrt{3}$ layer (Fig. 1, spectrum j) peak 1 falls off until at monolayer saturation it has almost completely van-

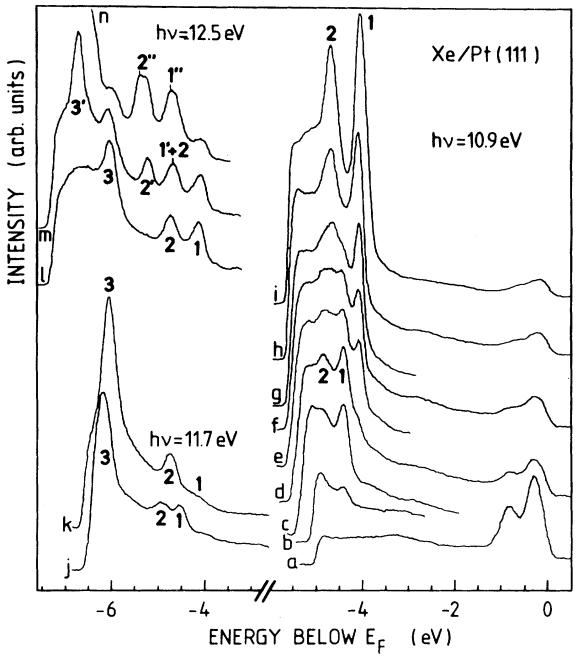

FIG. 1. Photoelectron spectra of xenon on Pt(111) for normal incidence and emission ($\Delta\theta = \pm 3°$). Peaks 1–3 are numbered with increasing binding energies and are explained in detail in Figs. 2 and 3. Right part: series of spectra taken at various coverages starting from (a) the clean substrate, ($b-d$) growth of $\sqrt{3}$ islands, ($e-h$) coexistence of $\sqrt{3}$ and hcp domains, up to (i) saturation of the full hcp monolayer. Left part: (j) completed $\sqrt{3}$ layer, (k,l) hcp monolayer, and (m, primed peaks) growth of second and (n, double primed) third layer.

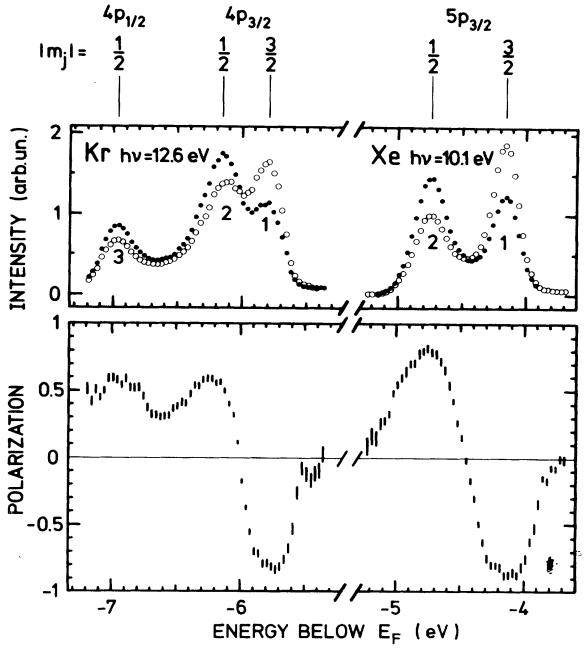

FIG. 2. Spin-resolved photoelectron spectra of Kr and Xe monolayers at full coverage. Upper part: intensities scattered into the two backward counters ($\pm 120°$) of the Mott detector, solid and open circles. Lower part: photoelectron polarization resulting from the scattering asymmetry normalized to complete circular photon polarization ($P = +1$ and -1 if electron and photon spins are parallel and antiparallel, respectively).

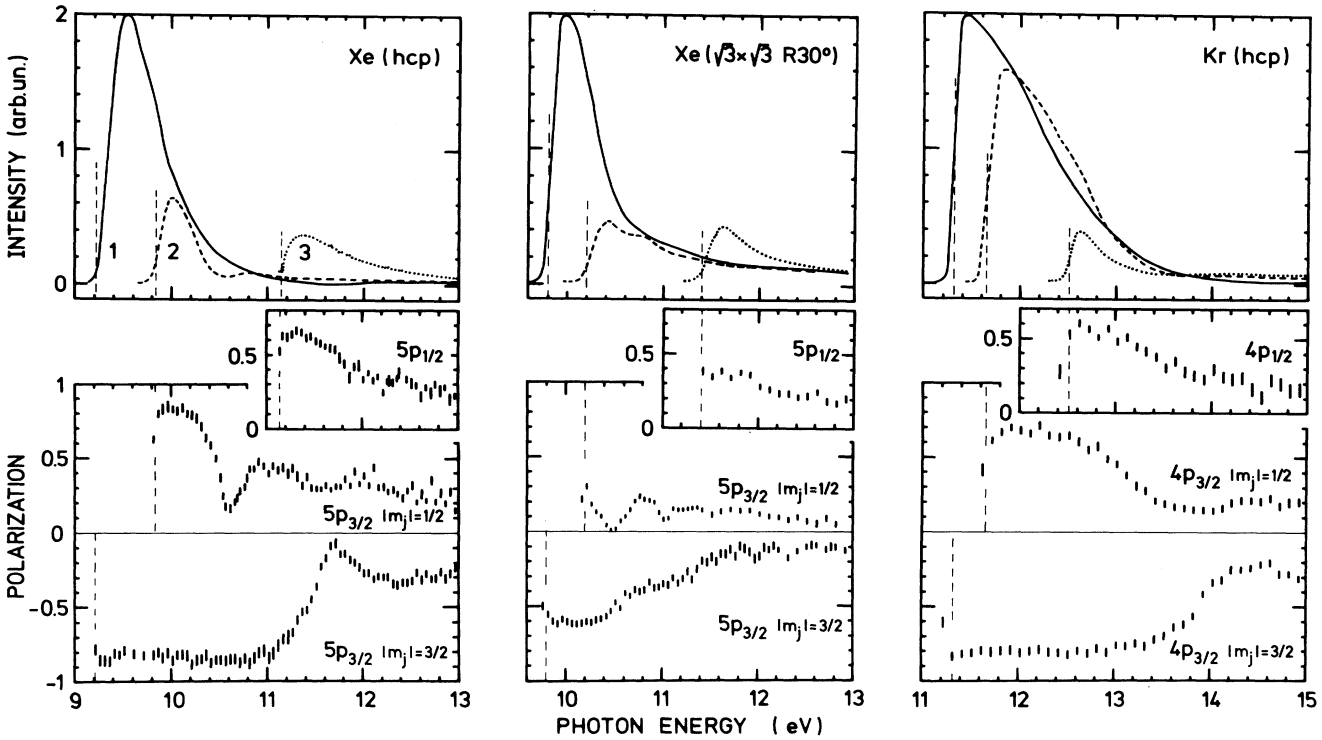

FIG. 3. Spectral variations of intensities (upper figures) and corresponding spin polarizations (lower figures) of the adsorbate photoemission peaks. Solid, dashed, and dotted curves correspond to $p_{3/2}$, $|m_j| = \frac{3}{2}$; $p_{3/2}$, $|m_j| = \frac{1}{2}$; and $p_{1/2}$, respectively. Vertical dashed lines denote threshold positions; the photon bandwidth was 80 meV at $h\nu = 12$ eV.

ished (spectrum k). *This example demonstrates that in the threshold region the peak heights are no longer a direct measure of coverage*—the dependence may even be reversed. Also the features in the second channel $p_{3/2}$, $|m_j| = \frac{1}{2}$ differ significantly for Xe hcp and $\sqrt{3}$. The variations for Kr are considerably broader.

The polarization curves can obviously not be explained entirely in terms of the quasiatomic picture which leads to Eq. (1). They are rather the result of an interplay between different mechanisms: (i) The energy-dependent *overlap between initial- and final-state wave functions* can cause strong variations of the radial dipole matrix elements including zero (Cooper) minima. (ii) *Interference of different partial waves* ($\epsilon s, \epsilon d$) of the outgoing photoelectron acts strongly on angular-distribution and spin-polarization patterns. (iii) *Discrete Rydberg-type or excitonlike excitations* may interact with an open photoemission continuum which leads in the gas phase to autoionization structures.[2] (iv) *Subsequent diffraction of photoelectrons* at the substrate or adatom lattice (both high-Z atoms) changes the spin-polarization significantly.[3] (v) *Resonances due to the surface barrier* induced by the image charge may occur, recently observed in spin-polarized LEED.[10] Process (iii) occurs if, e.g., a Xe $5d$ level (reached by a dipole transition) with excited core configuration $5p^5(^2P_{1/2})$ decays into the $|m_j| = \frac{1}{2}$ channel with ground-state core $^2P_{3/2}$ ($|m_j|$ conserved). This is most probably the origin of the polarization maximum around 10.9 eV in the $p_{3/2}$, $|m_j| = \frac{1}{2}$ channel for Xe hcp and $\sqrt{3}$ which is weakly visible in the intensities, too. That feature is preceded by a characteristic polarization minimum and appears for different Xe coverages, on a carbon contaminated Pt surface and also on graphite.

Being sensitive to weak interactions like phase shifts of wave functions,[1,2] spin-polarization measurements open a new and promising area in surface photoemission; for a detailed insight into the prevailing mechanisms a theoretical calculation would be highly desirable.

In conclusion, we have performed a first study of spin-polarized photoemission from atoms in the adsorbed phase. Very high photoelectron polarizations ($\pm 85\%$) occurred, exceeding all values previously found for other nonmagnetic solid-state systems. The signs of the polarizations provided a definite assignment of the Xe and Kr adsorbate valence levels. Attention was focused on the threshold behavior of the adsorbate photoemission where intensity and spin polarization show pronounced spectral variations versus photon energy, indicating the presence of strong dynamical effects.

We thank our colleagues A. M. Bradshaw, K. Horn,

and K. Kambe for many discussions and a critical reading of the manuscript, and J. Kirschner (Jülich), N. Müller (Osnabrück), and the BESSY staff for cooperation. This work was supported in part by Bundesminesterium für Forschung und Technologie.

[1]Ch. Heckenkamp, F. Schäfers, G. Schönhense, and U. Heinzmann, Phys. Rev. Lett. **52**, 421 (1984), and references therein.

[2]U. Heinzmann, J. Phys. B **13**, 4353 (1980) for Xe; F. Schäfers, G. Schönhense, and U. Heinzmann, Phys. Rev. A **28**, 802 (1983) for Kr and Ar.

[3]R. Feder, Solid State Commun. **21**, 1091 (1977), and **28**, 27 (1978).

[4]B. J. Waclawski and J. F. Herbst, Phys. Rev. Lett. **35**, 1594 (1975).

[5]K. Horn, M. Scheffler, and A. M. Bradshaw, Phys. Rev. Lett. **41**, 822 (1978).

[6]See, e.g., K. Wandelt and J. E. Hulse, J. Chem. Phys. **80**, 1340 (1984); T. Mandel, G. Kaindl, and W. D. Schneider, to be published; K. Jacobi and H. H. Rotermund, Surf. Sci. **116**, 435 (1982); R. Opila and R. Gomer, Surf. Sci. **127**, 569 (1983), and references therein.

[7]S.-I. Ishi and Y. Ohno, J. Electron Spectrosc. Relat. Phenom. **33**, 85 (1984).

[8]A. Eyers, F. Schäfers, G. Schönhense, U. Heinzmann, H. P. Oepen, K. Hünlich, J. Kirschner, and G. Borstel, Phys. Rev. Lett. **52**, 1559 (1984).

[9]B. Poelsema, L. K. Verheij, and G. Comsa, Phys. Rev. Lett. **51**, 2410 (1983), and to be published.

[10]D. T. Pierce, R. J. Celotta, G.-C. Wang, and E. G. McRae, Solid State Commun. **39**, 1053 (1981); P. J. Jennings and R. O. Jones, Solid State Commun. **44**, 17 (1982).